





Techniques, Tools, Platforms and Algorithms in Close Range Photogrammetry in Building 3D Model and 2D Representation of Objects and Complex Architectures

Massimiliano Pepe¹  and Domenica Costantino² 

¹Dicatech, Politecnico di Bari, via E. Orabona 4, Bari, Italy, massimiliano.pepe@poliba.it

²Dicatech, Politecnico di Bari, via E. Orabona 4, Bari, Italy, domenica.costantino@poliba.it

Corresponding author: Massimiliano Pepe, massimiliano.pepe@poliba.it

Abstract. The aim of this paper is to identify a suitable pipeline in order to build high-resolution 3D models and 2D orthophotos of objects and architectural structures of particular historical and cultural importance by means of the photogrammetric method. An accurate reconstruction of architectural elements can be exploited both for a detailed analysis of the artefacts, and also to determine the original position of detached architectural fragments. Structure from Motion (SfM) and Multi View Stereo (MVS) approaches have already been successfully applied in many applications to build 3D models. Moreover, the obtained reconstruction can be exploited in order to build orthographic projections of the object from different directions: the orthophotos generated in this way ensure a very high geometric resolution (even sub-millimetre) and accuracy. Orthophotos are particularly useful for the digital documentation and analysis of archaeological and architectural objects. To such aim, the direction to be used for the computation of the orthophoto, which in certain cases might be non-trivial, should be carefully determined. This work describes a simple procedure for the definition of such projection direction, while also enabling the express the object position according to certain specific requirements. In addition, the use of low-cost smartphone and action cameras was investigated to carry out photogrammetric surveys. Finally, this paper shows the results obtained with an imagery acquisition tool to be mounted on the top of a drone, developed ad hoc in order to properly acquire images for instance of the base of high bridges that cannot be achieved through a terrestrial survey. The developed tools and the overall proposed method is validated on three case studies, two related to terrestrial surveys, whereas the latter consider an example of UAV (Unmanned Aerial Vehicle) photogrammetry with the developed imagery acquisition device.

Keywords: SfM; Photogrammetry; MVS; CRP; orthophoto; CAD; UAV.

DOI: <https://doi.org/10.14733/cadaps.2021.42-65>

1 INTRODUCTION

Thanks to the recent technological developments, an increasing number of techniques and instruments can be used for Cultural Heritage (CH) digital documentation and for sharing the obtained representation. The documentation methods currently available can often lead to excellent results in terms of precision, speed, completeness and realism of the documented artefacts [1].

Recently, the combination of Close Range Photogrammetry and UAV (Unmanned Aerial Vehicle) platforms has become widely popular, leading to the introduction of the term "UAV photogrammetry" to identify such working condition [2].

The ease of application of SfM/MVS (Structure from Motion/Multi View Stereo) based 3D reconstructions, and to the automatism in the UAV flight planning and image acquisitions, this approach was applied in an increasingly number of contexts, ranging from architecture, architectural heritage, archaeology, geomorphology, to urban planning [3, 4, 5]. Since nowadays several drones are available on the market, the UAV platform selection can be done taking into account of the specific needs of the considered application, and of the different characteristics of the drones, such as control system, flight rules, the airspace classification, wing types, the take-off/landing direction, types of take-off/landing, aircraft engine, the fuel system, weight, maximum range of flight, flight altitude, aircraft functions [6].

The steps of the SfM-based photogrammetry processing pipeline can be summarized as follows: image pre-processing, key point extraction and match, computation of an initial solution for the exterior camera orientation parameters and 3D positions of tie points, bundle adjustment, dense point cloud generation and mesh building [7, 8], where the main steps of such procedure are typically performed by using the SfM and MVS approaches [9, 10, 11]. This processing pipeline has become popular mainly because of its ability to evaluate the camera's external orientation without any prior knowledge of the camera position and 3D points.

In the photogrammetric pipeline, sometime it is very difficult or impossible to build a correct 3D model from a set of pictures (shiny or transparent objects, moving objects, flat objects, etc.) This issue has led to the development appropriate sensors, techniques and algorithms capable of reconstructing 3D models [12, 13].

Once a 3D point cloud is computed, several other products can be produced, such as orthophotos. To be more specific, an orthophoto can be obtained as an orthogonal projection of points on a plane, consequently, different orthophotos can be obtained from the same 3D point cloud depending on the considered plane. The definition of the plane to be used for the orthophoto generation is rather intuitive, depending on the complexity of the object. For instance, in the case of a building, orthophotos can be generated in order to produce orthogonal views of its facades [14, 15]. Differently, the selection of a suitable plane for computing a proper orthophoto is a not so easy task when considering complex surfaces and objects. In order to ease such task, this work proposes a simple procedure based on a Lisp script that allows quickly and intuitively determining the parameters of the desired orthogonal projection in non-trivial cases.

Such procedure was tested on several case studies, along with an investigation of the 3D reconstruction performance obtained with low-cost cameras, such as those in smartphones and action cameras, with respect to that obtained with professional digital single-lens reflex cameras. Finally, an ad hoc imagery device was developed in order to acquire close views of certain parts of high structures, such as bridges, for photogrammetric purposes.

The paper is organized as follows. In the first part, the paper briefly summarizes the photogrammetric pipeline to be used to obtain 3D models and orthophotos. Then, a fast procedure developed in order to quickly determine planes to be considered for orthophoto generations is presented in the second part of the paper. Such procedure is tested on several case studies to check its effectiveness: the first case study deals with the 3D reconstruction of a small object using a standard smartphone camera. In the second case study, the survey and modelling of an architectural

element was realized using a compact camera. An extensible pole was also used in order to ensure a sufficiently detailed reconstruction of the upper part of the structure. In the last cast study, UAV photogrammetry was used for the survey of a roman masonry bridge. Since the base of the bridge was not accessible, a special device was realized to enable the UAV photo acquisitions of such part of the bridge from the bottom (in zenith direction). Finally, some conclusions are drawn at the end of the paper.

2 PHOTOGAMMETRIC PIPELINE

2.1 SfM Approach

The SfM pipeline allows the reconstruction of 3D object starting from a set of images acquired from different observation points by means of the following two steps [16, 17]: *Correspondence search* and *Reconstruction* stage. Furthermore, the first task can be divided in three sub-steps: Feature Extraction, Feature Matching and Geometric Verification. The Feature Extraction task, using suitable algorithm, such as the Scale-Invariant Feature Transform (SIFT) feature detector [18], allows to identify and describe local features and points of interest of the image in images (key-points). The Feature Matching searches for feature correspondences by finding the most similar feature task and identifies the parts of the images that are overlapping [19]. This Geometric Verification validates the potentially overlapping image pairs using a robust estimation technique, such as RANSAC (RANDOM Sample Consensus) [20].

As regards the Reconstruction stage, this stage can in turn be divided in four steps: Initialization, Image registration, Triangulation, Bundle Adjustment (BA). In the Initialization step, the system begins with a carefully selected two-view reconstruction and, in order to obtain a good reconstruction, it is desirable to start from an area containing a large number of the identified features. Subsequently, using feature correspondences, a new image is added to the reconstruction and, consequently, the corresponding camera position and orientation are calculated (Image registration step). This aim can be achieving by solving the Perspective-n-Point (PnP) problem [21, 22]. To define the 3D coordinates of the new points that can be added to the reconstruction and thus obtaining a denser point cloud, the Triangulation process is used. Lastly, Bundle Adjustment (BA) is used to improve the parameter values obtained in the initial SfM solution, e.g. improve the estimates of the camera poses. Extensive reviews on Bundle Adjustment and on the procedure to follow in order to achieve highly efficient reconstructions are given in several works [23, 24, 25, 26].

Brown (1971) [27] established a camera model widely used in photogrammetry: such model implements the collinearity condition to establish a mathematically rigorous relationship between image and object. It uses 10 additional parameters (Aps) related to internal camera orientation (Δx_p , Δy_p , Δc), uncertainty about the shape of the pixel (skew factor S_x), non-orthogonality of the reference system (shearfactor Λ), radial symmetric distortion of the lenses (k_1 , k_2 , k_3) and tangential distortion of the lenses (p_1 , p_2). The development of the so-called camera "self-calibration" allowed obtaining high 3D precision models also with low-cost (non-professionals) cameras. Two different approaches are typically used in the photogrammetric workflow: camera Self-calibration and Pre-calibration.

In the "self-calibration" approach, the internal parameters, external orientation and object coordinates of the points are unknowns. In this approach, the "Additional Parameters" (APs) are used to take into consideration of the systematic errors due to the acquisition process of the frames. Self-calibration with BA can be described by the extended collinearity model [20]:

$$\begin{pmatrix} x - x_p + \Delta x \\ y - y_p + \Delta y \\ -c \end{pmatrix} = \lambda \mathbf{R} \begin{pmatrix} X - X^c \\ Y - Y^c \\ Z - Z^c \end{pmatrix} \quad (1)$$

where

X, Y, Z	Object point coordinates;
X^C, y^C, Z^C	Perspective centre;
x_p, y_p	Principal point offsets;
$\Delta x, \Delta y$	Image coordinates perturbation;
R	Rotation matrix;
x, y	Image space coordinates;
c	Focal length (or principal distance);
λ	Scale factor for the image radius.

The additional parameters $\Delta x, \Delta y$ can be calculated by following equations:

$$\begin{aligned}\Delta x &= -\Delta x_0 + \frac{\Delta c}{c} \bar{x} + \bar{x} S_x + \bar{y} A + (k_1 r^2 + k_2 r^4 + k_3 r^6) \bar{x} + p_1 (r^2 + 2\bar{x}^2) + 2p_2 \bar{x} \bar{y} \\ \Delta y &= -\Delta y_0 + \frac{\Delta c}{c} \bar{y} + \bar{x} A + \bar{x} A + (k_1 r^2 + k_2 r^4 + k_3 r^6) \bar{y} + 2p_1 \bar{x} \bar{y} + p_2 (r^2 + 2\bar{y}^2)\end{aligned}\quad (2)$$

Where:

$\bar{x} = x - x_0$; $\bar{y} = y - y_0$ and $r^2 = \bar{x}^2 + \bar{y}^2$ while k_1, k_2, k_3 are radial distortion coefficients, p_1, p_2 are decentring (tangential) distortion coefficients, S_x the shape factor (uncertainty about the shape of the pixel) and A shear factor, i.e. the factor that takes into account of the non-orthogonality of the reference system.

The BA solution includes estimates of the external orientation parameters of each image and the object coordinates of the points, which are obtained by collimating a certain number of homologous points in all the images.

Instead, pre-calibration requires the introduction in the BA optimization of the internal camera parameter values as priors, which are pre-computed with a suitable camera calibration procedure.

An example of camera calibration software is Agisoft Lens that supports the estimation of the full camera calibration matrix, including non-linear distortion coefficients on the basis of Brown's model. Camera calibration procedure is typically obtained by properly processing a set of photos of a calibration pattern (chessboard) taken from different point of views. The typical outcomes of the calibration procedure are the estimated camera parameter values and their uncertainties, expressed as Standard Deviation values (SD).

2.2 Multi-View-Stereo Algorithms

Multi-View-Stereo algorithms, e.g., Clustering Views for MVS-CMVS and Patch-based MVS-PMVS [28] allow increasing the point cloud density previously generated during the SfM process. In this way, it is possible to produce accurate, coloured and point clouds much denser than the SfM-derived sparse ones.

MVS algorithms exist in several form: volumetric representations [26], PMVS implementation of Furukawa [29] and Multi-View Stereo for Community Photo Collections approach by Goesele [30], which reconstructs a depth map for every view.

2.3 Acquisition Technique in Close Range Photogrammetry Environment

The SfM-MVS approach allows the reconstruction of 3D structures starting from a set of images acquired from different observation points.

Typical characteristics of the camera network employed for automated close-range camera self-calibration are: acquisition of many images recorded with fixed zoom/focus settings, diversity in camera roll angles and views arranged in a strongly convergent configuration [20]. Indeed, the use

of a suitable image acquisition technique plays a fundamental role for the success of the SfM-MVS procedure.

For example, figure 1 shows a possible camera configuration for the reconstruction of the famous "Rubik's cube".

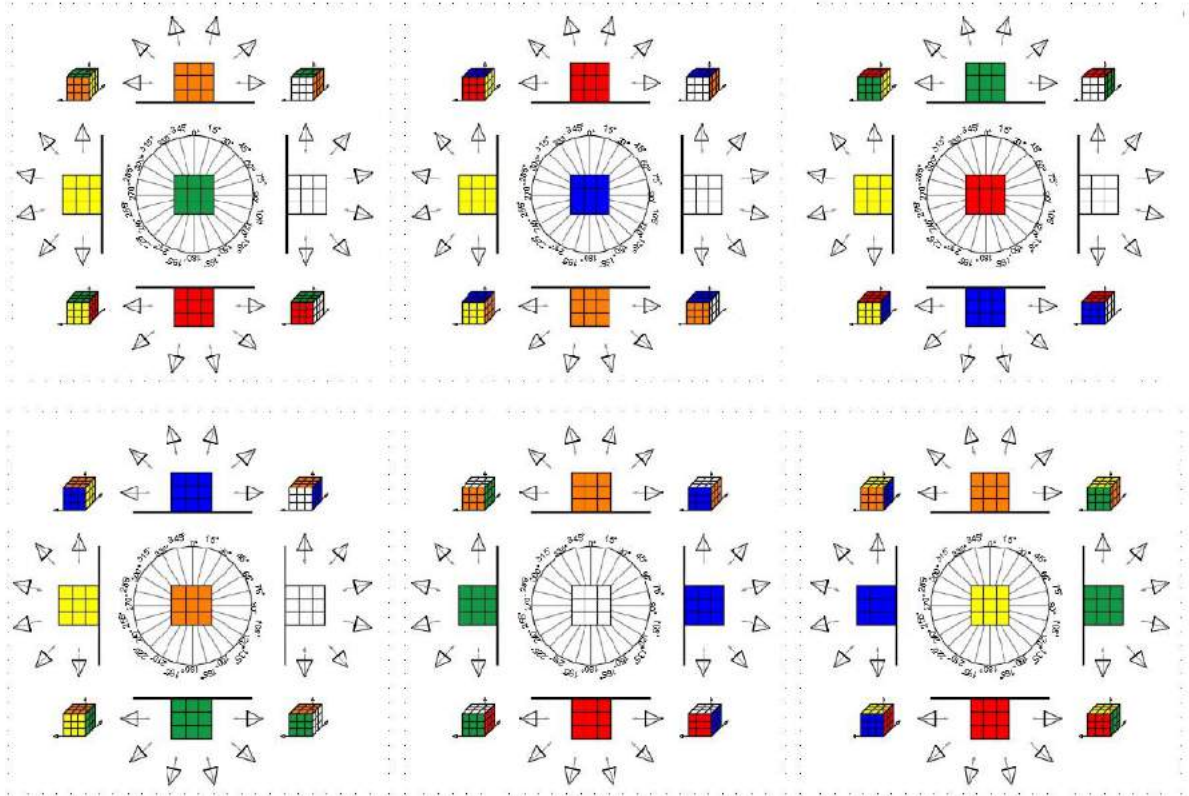


Figure 1: Examples of the appropriate capturing scenarios of the 3D object by SfM photogrammetric technique.

2.4 Surface Triangulation or Mesh Generation

Once a coloured dense point cloud is built, the construction of a polygonal surface (triangular or tetrahedral meshes) properly fitting such cloud is considered next. Using an appropriate triangulation process, a given set of points is converted into a coherent polygonal model. Such triangulation can be performed in two or three dimensions, in accordance with the geometry of the input data. A widespread two-dimensional interpolation method is the Delaunay Triangulation (DT).

Starting from the intuition of Dirichlet for the decomposition of a domain into several adjacent (and non-overlapping) convex polygons, the Delaunay method allows defining three-way points such that the circle surrounding each triangle does not contain other elements of the original point set [31]. A 3D Delaunay triangulation is also called a Delaunay tetrahedralization. A tetrahedral mesh is a discrete representation of a 3D continuous space, both in its topology and geometry [32]. In general, the conversion from point clouds into a polygonal surface is based on four steps [33]:

- pre-processing: the erroneous data are eliminated;
- determination of the global topology of the object's surface: the relations of the several parts of the feature are established;

- generation of the polygonal surface: triangular (or tetrahedral) meshes are created satisfying specific quality requirements;
- post-processing: editing and refining of the 3D model.

2.5 Orthophoto Generation

Orthographic projection (or orthogonal projection) is a means of representing three-dimensional objects in two dimensions. Therefore, in several applications one or more orthophotos of an object can be considered to properly describe it, where each orthophoto is associated to a properly selected plane. Depending on the quality of the orthophotos, a further editing in raster graphics editor software may be required.

2.6 Agisoft Metashape Pipeline and Possible Settings

Agisoft Metashape was used for 3D data processing in all the case studies investigated in this manuscript. In this software, the 3D model reconstruction and orthophoto can be obtained by following steps.

- (SfM) Image alignment. Homologous key-points are detected and matched on overlapping images, leading to an estimate of the external camera parameters. Before performing image alignment, the object of interest shall be separated from background ones using masks: such step allows to both reduce the computational effort, and to reduce the risk of matching errors, due to the changes in the surrounding environment in the images acquired by quite different points of view. Several accuracy options can be selected at this step: selecting "High" accuracy, Agisoft Metashape uses the full resolution photo, "Medium" setting causes image downscaling by factor of 4 (2 times by each side), at "Low accuracy" source files are downscaled by factor of 16, and "Lowest" value means further downscaling by 4 times more. Furthermore, "Key point limit" (upper limit of feature points on every image to be taken into account during current processing stage) and "Tie point limit" (upper limit of matching points for every image) can also be properly set.
- (MVS) Building dense cloud. By the use of dense image matching algorithm, the software generates a dense point cloud, whose final cardinality depends on the chosen settings: "Ultra high" setting implies the processing of full size images, whereas with "High", "Medium", "Low" and "Lowest" images are downscaled before the dense matching procedure by a factor 50%, 25%, 12.5% and 6.75%, respectively.
- Building mesh. In this step, textured triangulated meshes are obtained from dense point clouds. If interpolation mode is *Disabled*, the software leads to more detailed reconstruction results since only areas corresponding to dense point cloud points are reconstructed. Manual hole filling is usually required in a post-processing step. With Enabled interpolation mode Agisoft Metashape interpolates point positions within a neighbourhood of each point, defined by a properly set distance. As a result, some holes are automatically removed.
- Building orthomosaic. In this step, the whole object surface is textured in the orthographic projection. In addition, Agisoft Metashape enables to perform orthomosaic seam-line editing for better visual results.

3 METHOD

To build textured 3D models, the first step is to evaluate if the object (or structure) under investigation can be realized by terrestrial or aerial survey.

This aspect is related to dimensions of the object (or structure) especially in height. In this latter case, the use of a special pole may be useful to reach suitable heights for the survey. Instead, in the case the survey cannot be realized by traditional platform, special device must be realized in order to acquire information. For example, in order to perform a survey of structures located in critical environment (places not accessible by land or with imminent dangers for the operator or due to natural obstacles) the UAV platform may be modified in order to acquire

information to 360° of the scene. For achieve this aim, it is necessary to design of a special device that mounted on the top of UAV allows to observe a scene a 360; this involve in the use a further special camera (light. wide field of view) that requires an evaluation of the level of accuracy. This latter task may be obtained by the use of 3D test-field.

Therefore, once acquired the images by the use of suitable low-cost sensor and platform, using SfM/MVS approaches is possible to build 3D point cloud. Depending on the accuracy achieved in the specific case study, self-calibration or pre-calibration mode is used.

Subsequently, once obtained a textured 3D model as previously described, in several applications it is necessary to consider a representation of such objects obtained by means of one or more orthophotos. To such aim, a proper direction should be properly determined in order to obtain each desired orthographic projection of the reconstructed object. To ease the computation of such direction, a rigorous approach was developed in this paper, exploiting a CAD (Computer-Aided Design) software, as described in the following. This environment allows to easily identifying geometric conditions (e.g. parallelisms, orthogonality) in relation to the shape of the object and the plane you want to have as reference.

First, the specific plane along which the orthophoto shall be computed is identified by setting some GCPs (Ground Control Points) on the images in Agisoft Metashape. Then, GCPs and the 3D point cloud (preferably the sparse point cloud because it is easier to manage), which are typically expressed in a UCS (User Coordinate System) i.e. the mobile Cartesian coordinate system that defines the work plane, are imported in CAD environment.

The import of the GCPs within the CAD environment were obtained through the development of appropriate algorithms developed in Lisp (List Processor) language, which is a programming language developed by McCarthy [34] and used in Computer-Aided Design (CAD) systems [35]. The use of GCPs arranged along the desired axes allows obtaining a proper rotation and translation of the 3D object. From an analytical point of view, the rotation in the space of each point P with coordinates (x,y,z) in a generic coordinate system, in a desired coordinate system (X,Y,Z) can be obtained using the cosines of the angles between the coordinate axes [36]:

$$\begin{pmatrix} X \\ Y \\ Z \end{pmatrix} = \begin{pmatrix} \cos(xX) & \cos(yX) & \cos(zX) \\ \cos(xY) & \cos(yY) & \cos(zY) \\ \cos(xZ) & \cos(yZ) & \cos(zZ) \end{pmatrix} \begin{pmatrix} x \\ y \\ z \end{pmatrix} \quad (3)$$

In the synthetic formula, the previous formula can also be written as:

$$X = R\mathbf{x} \quad (4)$$

The rotation matrix R consists of 9 linearly independent parameters generated by 3 variables in a non-linear way. Each row and each column of the rotation matrix must have unitary value, and each row and each column are orthonormal to each other, as they form an orthonormal basis.

Subsequently, only the GCPs are exported according to the new reference system and imported into the SfM software in order to build the orthophoto and, of consequence, to obtain CAD representation of a façade (or a particular) of the object (or structure) too.

In our experimentation, we used Agisoft Metashape commercial software but the same approach can also be applied to other commercial and non-commercial 3D photogrammetric software. The aspect to take into account is the possibility of the software to import and export GCPs according to a specific formatting of the file.

In summary, the developed pipeline that allows obtaining 2D representation (orthophoto) from 3D model is shown below (Figure 2):

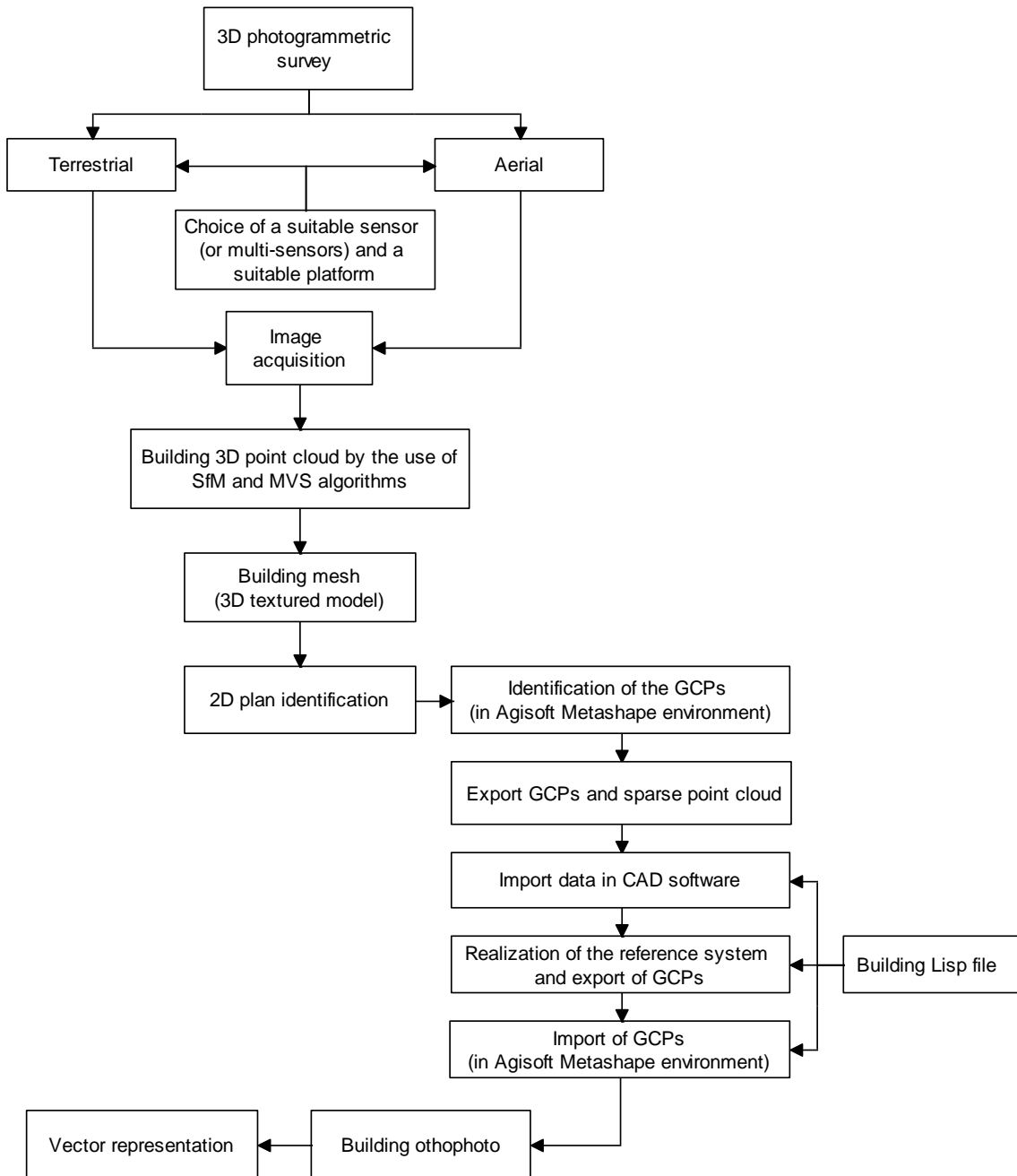


Figure 2: Pipeline to obtain 3D model and 2D orthophoto-Vector representation.

The method described was applied to three case studies. The first one concerns the modelling of a mortar of modest dimensions and surveyed with terrestrial photogrammetry. The second case study concerns the construction of a 3D model of an ionic capital inside an archaeological area and surveyed with terrestrial photogrammetry and with the aid of a pole (to survey the upper part of the

structure). The third case study concerns the modelling of a historical masonry bridge surveyed by photogrammetric method, in its entirety, exclusively with UAV platform.

4 CASE STUDIES

4.1 Case Study 1: 3D and 2D Representation of a Stone Mortar

4.1.1 3D survey and modelling

This case study investigates the reconstruction and representation of a stone mortar. Mortars were used since ancient times to prepare ingredients or substances by crushing and grinding them into a fine paste or powder in the kitchen, medicine and pharmacy. The mortar used in this case study is a hand-carved marble stone from Italy, probably dated back to the late 19th century, whose sizes are: 18 cm diameter across the handles/lugs, by 16 cm the high and 3cm the thick.

The photogrammetric surveys of this object were carried out using Huawei P20 lite smartphone that is a low-cost device able to acquire images with a resolution of 16MP with a f/2.2 lens. The pixel dimension of Huawei P20 lite smartphone is of 1.1 μ m and the focal length is 3.81mm. 156 images were taken at a distance of about 30 cm and using the same focus in order to obtain a GSD (Ground Sample Distance) of about 0.1mm.

Four sessions of survey were performed because for 4 times the object was rotated in order to properly acquire all its details. In each session, the photos were taken with a convergent arrangement, as suggested for SfM surveys of isolated objects. As background, a black panel was used in order to ease the mask definition process. Indeed, in this way, the high contrast between the object and the background, allowed an effective use of the border recognition tool (that it is implemented in the software with the name "intelligent scissors"), allowing the draw of the polygon of the area of interest on the image in a quick and accurate way. In addition, the survey was performed in an open environment with uniform lighting condition on the object.

In the alignment step, all the images were correctly positioned in the space and a sparse cloud of 320,872 points was generated. The dense cloud was generated using the setting "high", which lead to the computation of 3,192,236 points. A representation of the position of the cameras on the point cloud that schematically shows the acquisition pattern is shown in Figure 3a. In building mesh, using "moderate" parameter as "Depth filtering" and enabling the interpolation, 6,313,344 facets were created. Table 1 shows the error evaluated on 4 calibration bars.

Scale bar	Dimension (m)	Error (m)
1-2	0.20	0.0005
3-4	0.20	0.0002
5-6	0.20	0.0001
7-8	0.20	0.0004

Table 1: Accuracy of the photogrammetric block of the images.

The total error, i.e. root mean square error for X, Y, Z coordinates for all the cameras can be calculated by following formula:

$$\text{total error} = \sqrt{\sum_{i=1}^n \frac{(x_{i,est} - x_i)^2 + (y_{i,est} - y_i)^2 + (z_{i,est} - z_i)^2}{n}} \quad (5)$$

Where x_i is the input value for x coordinate, y_i the input value for y and z_i the input value for z coordinate for the i -th camera position, while $(x_{i,est}, y_{i,est}, z_{i,est})$ corresponds to its estimated position.

Using the setting *highest*, the total error achieved was 0.0002m. Varying the level of accuracy available within the software, it was possible to build the following Table 2. In this way, it is possible to identify the quality of the alignment according the diverse resolution of the photo. In addition, an analysis of the processing times was carried out in order to analyse the different settings (available within the software).

Level of accuracy	Aligned images	Total error (m)	Cover of the object	Time processing (s)
Highest	156/156	0.0002	Full	7926
High	156/156	0.0002	Full	7067
Medium	154/156	0.0003	Full	1551
Low	154/156	0.0003	Full	340
Lowest	59/156	-	Partial	97

Table 2. Evaluation of the accuracy varying the alignment setting.

The final 3D model with mesh can be visualized according three type of representation: solid (figure 3.b) and coloured mesh (figure 3.c) views

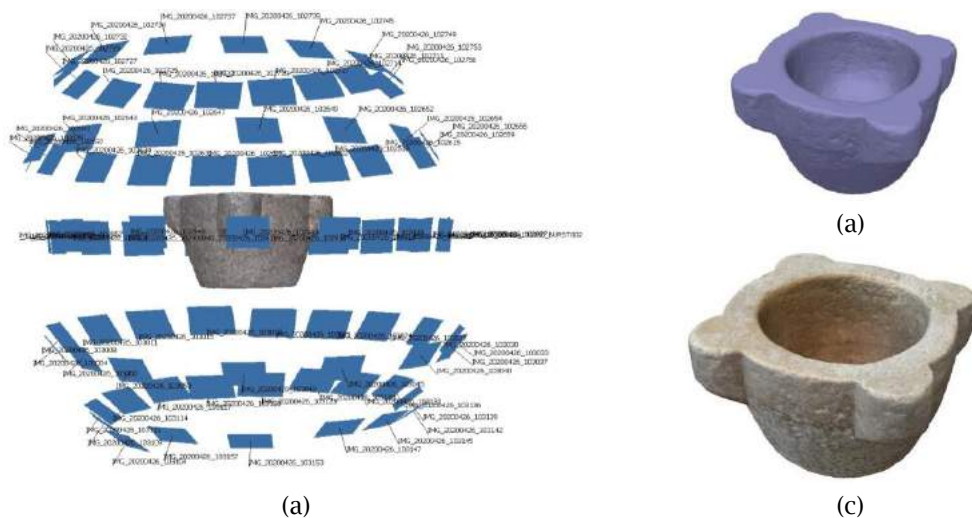


Figure 3: 3D models: View of point cloud and cameras poses (a); 3D model in solid view (b); 3D model with texture (c).

The same object was also detected with a Nikon D5000 digital Single-Lens Reflex (dSLR) camera with a AF S DX NIKKOR 35mm f/1.8G lens. 149 images were acquired and, subsequently, processed in Agisoft Metashape software. In this test, the total error achieved was 0.00002m. This means that the use of dSLR cameras and quality lenses allows high accuracy to be achieved.

4.1.2 2D representation

The produced 3D model is typically positioned and orientated according to a generic reference system. In other words, the base of the object is not parallel to the horizontal axis. In order to achieve this aim, the pipeline indicated in figure 1 was carried out. Indeed, 6 GCPs were created in

SfM software and, subsequently, exported in *.csv format. Similarly, the sparse point cloud in .dxf format was exported. It was chosen the sparse point cloud because the management of a small point cloud was easier. Then, the point cloud and the GCPs were imported in CAD environment. Once established the new reference system, the new coordinates of the GCPs were exported and used in Agisoft Metashape software. In this way, it was possible building the orthophoto (2D) of the single façades of the object. Indeed, using the mesh as surface and the option "Mosaic" as "Blending mode", the orthophoto with a resolution of 0.2mm was generated using the tool Building orthomosaic. To improve the quality of the orthophotos, an editing in Photoshop CS5 was carried out. Indeed, this software has a complete toolbox for retouching and colour correction, and it allows importing and managing individual orthorectified images in separate layers. A 2D representation of the surveyed stone mortar is shown in the figure 4.

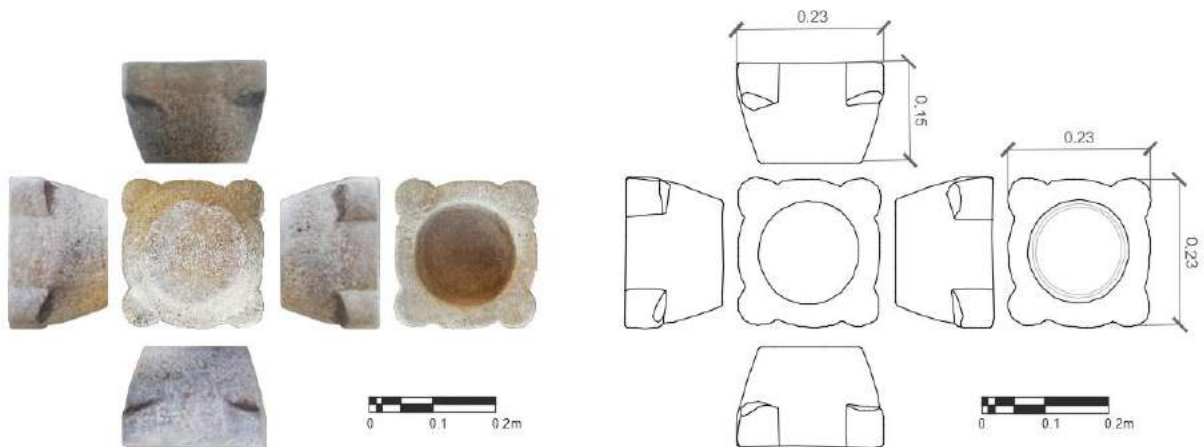


Figure 4: 2D representation of the object under investigation.

4.2 Case study 2: survey and modelling of the Ionic capitals located in the archaeological area of Metapontum, Italy

4.2.1 3D survey of a capital in Metapontum area

The second case study concerns the capitals and the related colonnades in the archaeological area located in Metapontum, in the south Italy (figure 4.a).

This area includes the urban sanctuary, part of the agora, the handicraft district for the production of ceramics, the great north-south road axis (*plateia*) on which the entire urban system is imposed and the temples. This latter structure represents the most important testimonies for the knowledge of the contributions of the Greek oriental world to the architecture of the Greek west in the late archaism and in the early classical age. Among the four main temples of the sacred area, the largest two have been attributed to *Hera* and *Apollo*; the *sacellum* is considered consecrated to Athena while the fourth temple is considered to belong to *Artemis* or, according to another hypothesis, to *Aphrodite* [37].

The capitals and the related colonnades of this latter temple were taken into consideration in the present study, in relation to their state of conservation and the particular shapes of the structures. In particular, the centre capital of East side was surveyed.

As shown in figure 5, at the base of the columns, there are metallic (artificial) structures that have allowed to bring back the original structure to their exact position. In this way, verticality was given to the colonnade and a horizontal position to the capitals and to the structure resting on them.

In other words, a physical roto-translation of the structure was made with respect to the position in which they were located.

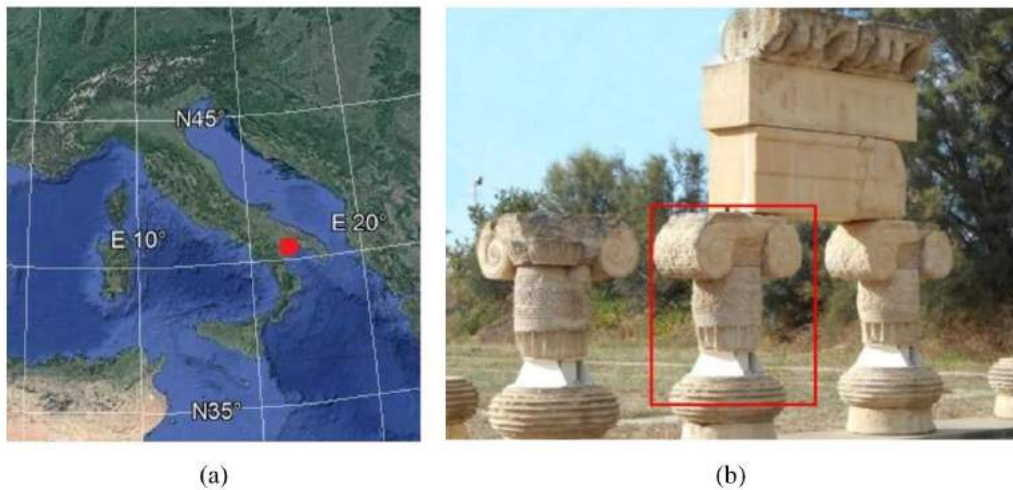


Figure 5: Study area: Identification of the Metapontum site (Italy) on Google Earth map - approximated geographic coordinates, latitude: 40.383570°N, longitude: 16.824375° E (a); panoramic photo of the structure and identification of the capital under investigation (b).

The survey of the capital was realized using ultra-compact camera Canon PowerShot SX730 HS. The Canon PowerShot SX730 HS features a 20.3 megapixel 1/2.3-inch CMOS sensor, and a 40x optical zoom which is equivalent to 24-960mm in 35mm terms. In particular, the survey of the lower part was performed with this camera according to the CRP approach. Since the upper part is not detectable through a traditional photogrammetric survey, it was necessary to use a pole extensible for maximum length of 4 meters. The pole is composed by an extensible rod and a device positioned at the end of the pole where the camera is fixed. A total amount of 217 images were acquired and the processing was carried out in Agisoft Metashape software. In this way, a textured 3D model of the Ionic capital was realized. The output parameters of the elaboration in Agisoft Metashape software, can be summarized in the following Table 3.

<i>Features</i>	<i>Values</i>
Tie points (#)	420,312
Dense clouds (#)	6,147,741
Faces (#)	11,622,989
Total error evaluated on 3 scale bar (m)	0.0006

Table 3: Output parameters of the project.

4.2.2 2D representation: orthophoto and vector (traditional approach)

Considering the complexity of the structures taken into consideration, ten GCPs (easily recognizable) on the structure were used. In order to carry out the roto-translation, a specific plane was chosen. In this way, it was possible to build an orthophoto with a spatial resolution of 0.2mm (Figure 6).

Figure 7 shows a 2D representation of the Ionic capital where on the left image, it is shown the detailed orthophoto (figure 7.a) while on the right image, it is reported a vector representation of the external façade of the temple (figure 7.b).



Figure 6: Textured 3D model and definition of the plane on the capital.

This latter representation was obtained through the aid of “edge detection” algorithm, which is the process of locating brightness discontinuities between pixels in a digital image. In particular, Sobel operator was used for obtaining a vector representation. Sobel is a discrete differential operator that utilizes two 3x3 kernels: one estimates the gradient in the x direction while the other one estimates the gradient in the y direction.

If we define A as the source image, the computations are as follows [38]:

$$\mathbf{G}_x = \begin{bmatrix} -1 & -2 & -1 \\ 0 & 0 & 0 \\ +1 & +2 & +1 \end{bmatrix} * A \quad \mathbf{G}_y = \begin{bmatrix} -1 & -2 & -1 \\ 0 & 0 & 0 \\ +1 & +2 & +1 \end{bmatrix} * A \quad [6]$$

where $*$ denotes the 2-dimensional convolution operation.

At each point in the image, the resulting gradient approximations can be combined to give the gradient magnitude:

$$G = \sqrt{G_x^2 + G_y^2} \quad [7]$$

Since these procedures calculate a local gradient, a threshold value was defined in order to discriminate noise and small variations from those to be considered in the vector representation. In this way, using Matlab software and suitable algorithms, a new image was generated.

This image was used as background in AutoCAD software (developed and marketed by Autodesk Company); in this way, the quality of the vector representation was checked and corrected, where needed (Figure 7.b).

4.3 Case Study 3: UAV Photogrammetry in Building 3D Model of a Masonry Bridge

4.3.1 Zenith UAV photogrammetry by the use of an ad-hoc device and action-camera

UAV photogrammetry provides a fast, precise, and cost-effective tool for surveying structures, quarries, cultural heritage sites, etc. In this way, it is possible to overcome the limits of the terrestrial survey. A frame camera is usually positioned under the UAV and, by the use of a gimbal, it allows

to obtain nadir and panoramic images. In addition, the gimbal allows the stabilization of an object on one or more axes too. For example, in a configuration without gimbal the camera is fixed with the body of the drone and, consequently, it follows all its movements and oscillations, causing the degradation of the acquired image quality. Instead, a 3-axis gimbal can be used to stabilize the camera on all three axes and prevent roll, pitch and heading movements from being transferred to the camera.

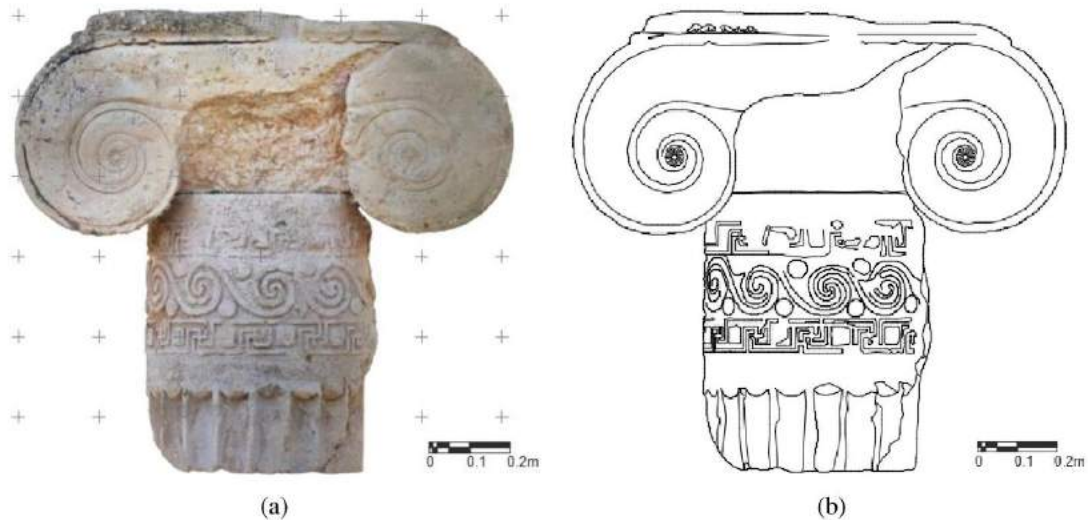


Figure 7: 2D representation of the external façade of a capital belonging to temple: Orthophoto (a); vector representation (b).

The camera tilting angle typically ranges from 0° to 90° , i.e. from nadir orientation to the horizontal one. Hence, it is impossible to observe objects positioned at a height greater than that of the UAV. Such working condition holds during the survey of several structures, such as domes, bridges, etc. Certain areas of such structures are usually not terrestrially accessible, hence aerial solutions such as platforms integrated with UAVs have recently been developed, e.g. Parrot Anafi drone. However, despite Anafi represents a viable way for visual inspections, recent tests have shown that it is not an appropriate solution for photogrammetric purposes [39]. For this reason, one of the aims of this paper is the development of a low-cost system able to acquire images of a structure from below, with zenith-oriented photos. In this way, it is possible to acquire information on high structures that, with traditional methods, would not have been possible or very expensive.

To realize photo from UAV in zenith direction, it was necessary to build a suitable low-cost system able to achieve this aim. The first objective concerned the choice of a suitable camera. Since such sensor has to be mounted on the UAV for photogrammetric purposes, it has to meet the following requirements:

- **Lightness:** due to the additional weight represented by the sensor, the UAV motors must be able in three critical situations:
 - lift the UAV without problems;
 - stay in the hovering position without perturbations;
 - stay in the air as long as possible. Indeed, the greater the weight of the sensor, the greater the effort of the motors and, consequently, the greater the battery consumption. This leads to a decrease in flight autonomy. So, the lighter the sensor, the lower the impact on the engines;

- remote controllable (being manageable from the ground): the possibility of being able to observe in real-time the scene object of the survey allows optimizing the execution times, e.g. to better frame the objective, to verify the correct exposure of the photo;
- sharp images even in critical conditions: since the images are captured from aerial platform, their quality can be affected by drone movements. The stability of the sensor can be obtained by means of electronic devices.

To achieve this aim, a special hardware provided with the action-cam was positioned on a plate in a stable and secure way. In turn, this plate was fixed on another plate through 4 shock mounts arranged symmetrically and at the edges of the plate. These shock mounts allow damping of vibrations induced by the UAV platform. In this way, the images generated by the sensors are sharper because they are less affected by sudden movements of the camera. The design of the system architecture (see figure 8a) was realized in Solidworks, a parametric three-dimensional drawing and design software, produced and marketed by Dassault Systèmes. The realization of the architecture is shown in the figure 8b.

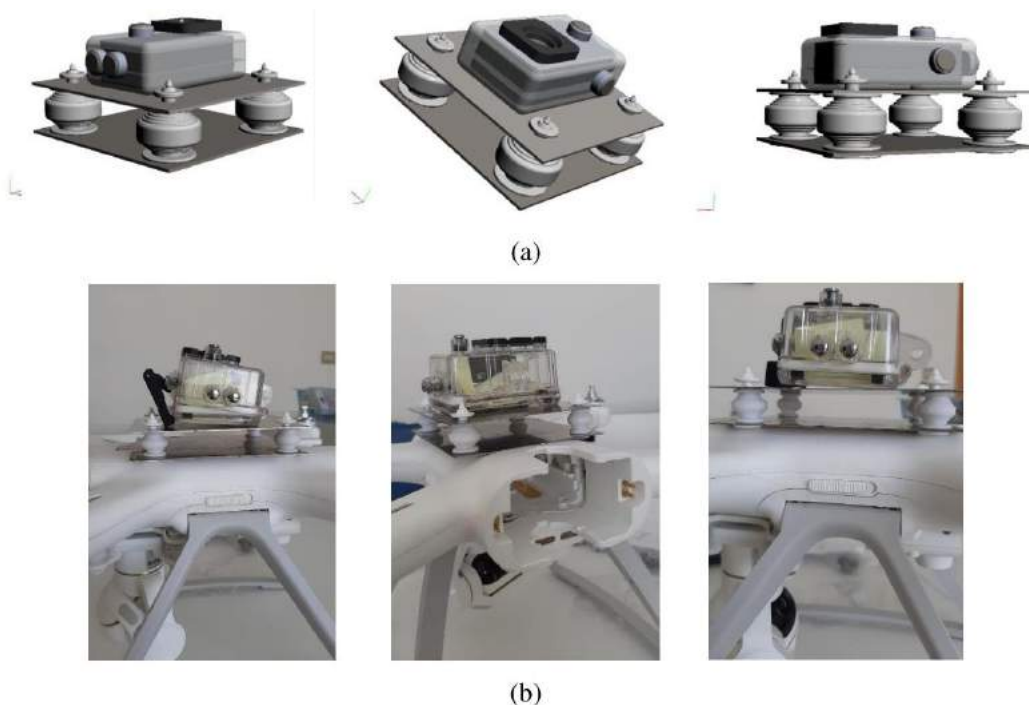


Figure 8: Architecture of the system: design (a) and realization (b).

The camera used for the several experimentations is the GoPro Hero3 Silver due its lightness. GoPro Hero3 Silver has a sensor to acquire images at a maximum resolution of 11Mp (format 3840x2880 pixels). This camera is able, even in backlighting, to reproduce colours faithfully: this means that this device allows excellent automatic exposure. The most important feature of this camera is the very wide-angle sensor (170-degree) that produces very important distortion on the image. Since that the action-camera sensors produce high distortions in the image, this involves an image construction that differs from the ideal model of central perspective (pinhole camera model) and, of consequence, reduce the quality of the accuracy. To reduce the impact of the distortions in photogrammetric approach, more tests were carried out in order to identify the best procedure that minimize the errors in the matching and alignment phases. Indeed, four scenarios that taking into account, or not, of the pre-calibration and/or the pre-correction of the lenses were realized. In particular, building a 3D test field, several test varying the features of the images were carried out.

In this way, it is possible to evaluate the Level of Accuracy (LoA) on 3D test field in the different scenarios. The analysis on achievable accuracy were performed using SFM/MVS approach. Nowadays, this approach is widespread in order to build 3D models and requires a block of images with a high degree of overlap that capture the complete 3D structure of the scene viewed from several positions [40].

The 3D test field was composed by 20 circular coded targets positioned at different heights from the ground and distant from each other of 20cm.

The level of accuracy achievable by this sensor was evaluated building four scenarios:

- Self-calibration;
- Self-calibration with radial distortion correction: before performing the alignment step, the images was corrected by radial distortion. This latter task was realized using a special tool developed in Adobe Photoshop software. Indeed, Adobe Photoshop software contains a large database of the filters for lens correction, including the "GoPro Silver" action-cam model. Since Photoshop allows batch operations, automatically and quickly, all the images were corrected, consequently reducing the barrel distortions on the images.
- Pre-calibration: in this scenario, the first task was to calculate the internal parameter. The software used for the camera calibration is Agisoft Lens. In this environment, it was possible to calculate coordinate of the principal point and radial lens distortions in the Brown's model. Of consequence, it was possible to plot the curves representing the radial and tangential distortion (Figure 9). As expected, the radial distortion curve goes upward to indicate that the lens has a barrel distortion type, and it sensibly increases its trend with respect to the radius, due to the wide-angle lens of this camera.

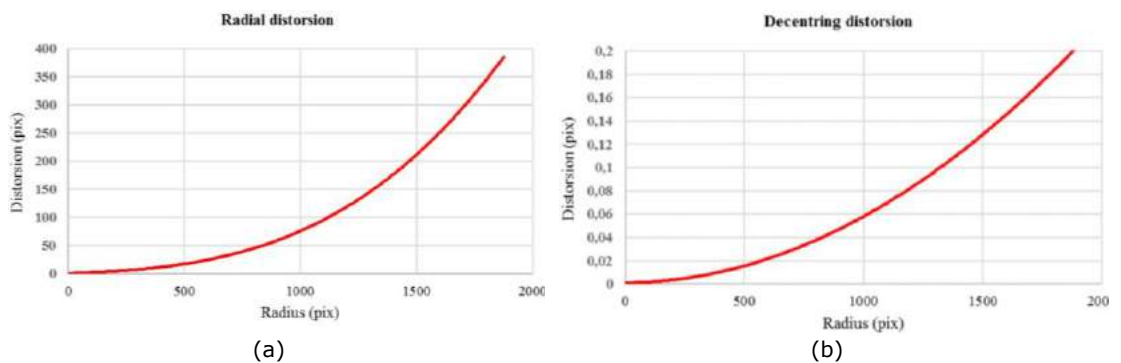


Figure 9: Plot of radial distortion (a) and decentring distortion (b).

- Pre-calibration with radial distortion correction: in this latter case, beyond use the calibration parameters, the radial distortions were corrected in the images.

The results of the several scenarios are shown in the following Table 4.

	<i>DATASET</i>	<i>Total Error (m)</i>	<i>Total Error (pixel)</i>	<i>Matching time</i>	<i>Alignment time</i>
1	Self-calibration	0.0009	2.796	11m 11s	3m 14s
2	Self-calibration with lens correction	0.0008	2.613	13m 14s	1m 53s
3	Pre-calibrated	0.0009	2.583	13m 21s	1m 32s
4	Pre-calibrated with lens correction	0.0007	1.163	12m 13s	1m 29s

Table 4: Time and accuracy achievable in the different scenarios.

As show in the table 4, the images corrected by radial distortions and using the calibration values obtained through the procedure described in the scenario n.4 showed a higher level of accuracy than the other scenarios and, at the same time, tight alignment times.

The survey of the 3D-test field was repeated using the Pentax K-5 that is a 16.3-megapixel digital single-lens reflex camera equipped with SMC Pentax-DA 35mm F2.4 AL lens. In particular, 39 images were captured. The post-processing of the images within SfM/MVS software allowed to obtain a total error of 0.3mm. Therefore, considering the high accuracy achievable with this sensor, the point cloud generated in this way, can be considered, as reference in order to compare the point clouds obtained with the different scenarios.

The comparison between the different point clouds was carried out using CloudCompare software [41], which is a 3D point cloud processing (open source) software but it can also handle triangular meshes and calibrated images. Before performing the comparison, a “cleaning” operation to identify and exclude outlier points that can negatively influence the results, was performed.

A common way to visualize the difference between the point clouds is based on the use histogram, where on the horizontal axis is reported the distance while on verticals axis is reported the number of values in a specific class. In addition, on the discrete diagram can be built and visualized the Gauss distribution (Figure 10).

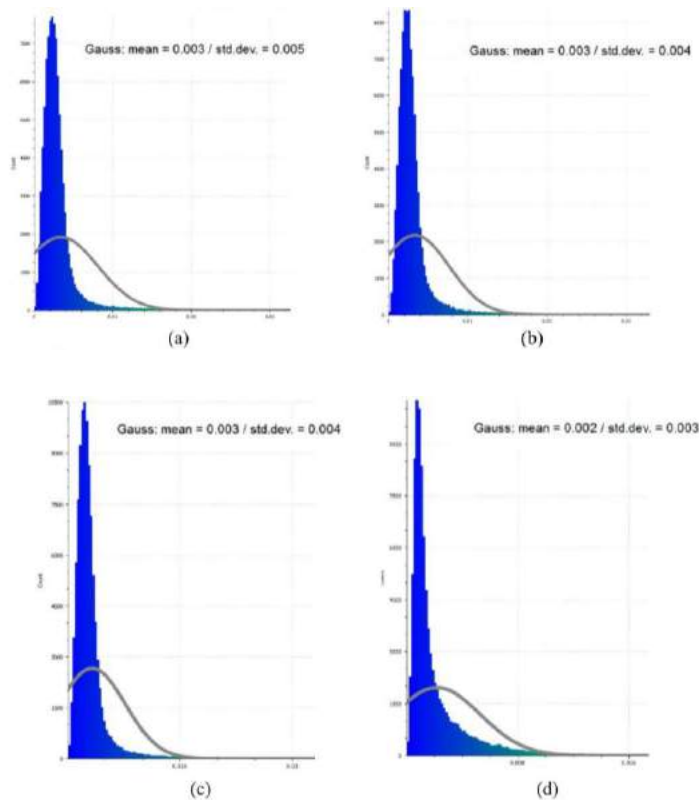


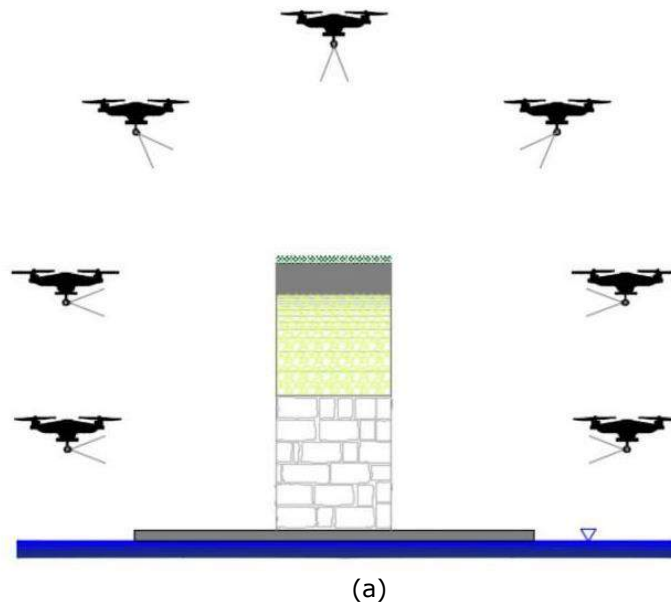
Figure 10: Histograms of the C2C between point cloud obtained by DSLR sensor (reference) and the several scenarios (compared) a) C2C between DSLR sensor and point cloud using “Self-calibration” dataset; a) C2C between DSLR sensor and point cloud using “Self-calibration with lens correction”; c) C2C between DSLR sensor and point cloud using “Pre-calibrated” interior parameters; d) C2C between DSLR sensor and point cloud using “Pre-calibrated with lens correction”.

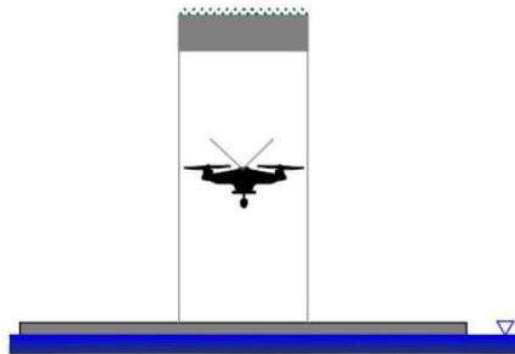
From the figure 10, it is possible to note as the best result was obtained in the case d), i.e. using the dataset "Pre-calibrated with radial correction".

4.3.2 Survey and 3D modelling of Annibale's bridge

The masonry bridge used for UAV photogrammetry test is located in southern Italy (approximate geographic coordinates: 40.643978, 15.483073), in the Platano river, in a narrow and not easily accessible canyon. It is also known as Annibale's bridge, probably to attest to the memory of the passage of the condottiere to which its construction is traced. The bridge is kept in fairly good condition, while showing signs of interventions performed over time. The bridge has a pronounced donkey-back profile with two arches, of which the larger one is much larger with a light of 12.65 and another smaller one of about 4.60 m. The total length of the bridge is about 30 m with a width of 3.40. Both the inner nucleus and some vestments (probably the work of successive restorations) are in opus caementicium while the shoulders and the piles (which seem ancient) have opus quadratum vestments. The survey was carried out using Xiaomi Mi Drone 4K, a multi-copter rotary wing type that allows achieving a max flight speed of 18 m/s with a max climbing speed of 6 m/s and lowering speed of 1.5 m/s. The drone is supplied of a digital camera able to acquire images with a resolution of 8.2Mpixel where the pixel size is 4.54 μm . The mission planning was divided in two parts: nadir-oblique and zenith direction (Figure 10). Indeed, the upper part of the bridge was planning in the way that the camera supplied with the UAS (Unmanned Aerial System) observes the bridge by nadir and oblique views. The flight planning was designed using Mission Planner software. 7 Flight Lines (FLs) along the longitudinal direction of the bridge was created. In order to cover entire structure according the basic principles of the survey technique based on the SfM approach, it was necessary varying the tilt angle, as shown in the Figure 11.a. In addition, the flight planning was realized using suitable values of (longitudinal) over-lap and (transversal) side-lap of the images [39].

To survey the upper part of the bridge, i.e. the intrados of the masonry bridge, zenithally photos were carried out, as shown in the figure 11.b. Therefore, a FL was planned and acquired in manual mode varying the flight heights in order to obtain (approximately) the same GSD.





(b)

Figure 11: Sketch of flight planning on the central section of the bridge (realized in CAD environment): flight planning to take nadir and oblique photos (a); flight planning to take zenithally photos (b).

In particular, three sessions of aerial survey were performed which two to realize the upper part of the bridge (nadir and oblique) and one to realize the photos in zenith direction. The photogrammetric flight allowed obtaining 345 images from the camera supplied with the drone and 175 with the action camera for a total amount of 520 images.

The images were imported in Agisoft Metashape software and processed in two datasets: one generated by action-camera sensor and another by the camera supplied with the drone.

While the dataset with the images acquired by the camera supplied with the drone was processed in self-calibration mode, the dataset of the images acquired by action-cam sensor was processed in pre-calibrated mode with radial correction of the single image. In this way, all the images were correctly aligned in each dataset. According to the photogrammetric pipeline was built the dense point cloud in both datasets.

Subsequently, in a new dataset, the point clouds were aligned by common points to both datasets. Once obtained a unique point cloud of the area under investigation, it was possible to build the textured mesh consisting of 2,362,420 faces.

The evaluation of the accuracy was carried out using suitable GCPs positioned on the top of the bridge and some natural points. The GCPs were measured by Total Station and, then, calculated by apposite tool developed in Matlab in order to transform the polar coordinates in a local Cartesian reference system.

Finally, it was possible to scale the model and, at the same time, obtaining a measure of errors in building 3D models. The total error achieved was about 10 mm.

The representation of the 3D model of the Roman masonry bridge obtained by photogrammetric method is reported in Figure 12.

By choosing appropriate GCPs on the structure, defined the planes on which to create the projection and using the developed procedure it was possible to build the orthophoto of the plan (from the top view) and the two lateral façades of the masonry bridge.

The GSD of the orthophotos (plan and façade of the bridge) was 0.5 mm.

The orthophotos realized in this way were arranged, subsequently, according to an architectural layout, where the plan is placed in the middle and the two extremes of the façades of the masonry bridge, as shown in the Figure 13.



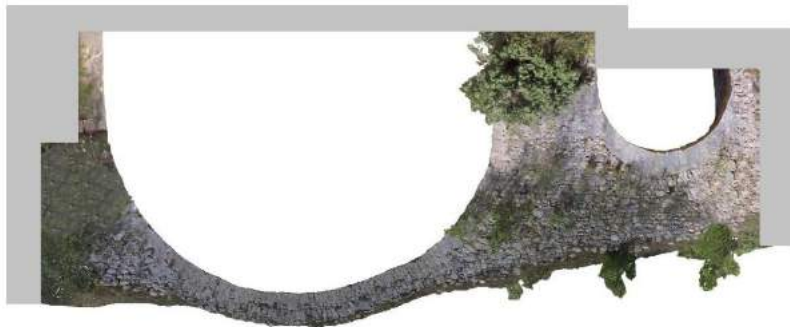
Figure 12: 3D model of the Roman masonry bridge.



(a)



(b)



(c)

Figure 13: Layout of the 2D orthophoto of the bridge: façade (a), plan from the top view (b) and other façade of the bridge (c).

In addition, it was possible to obtain the orthophoto from the bottom to the top and, of consequence to identify the discontinuity lines of the masonry of the intrados, as shown in the figure 14.

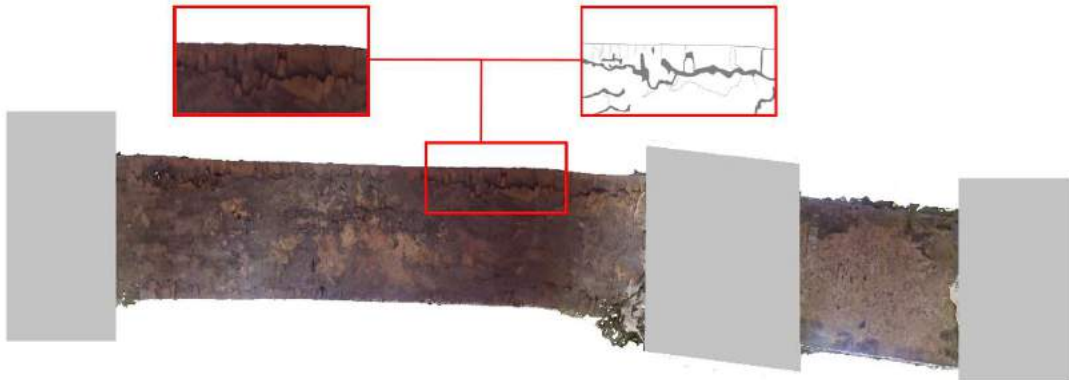


Figure 14: 2D orthophoto (plan) of the intrados of the bridge with the detail of the area where cracks are visible.

5 CONCLUSIONS

The combined use of a low-cost sensor, a suitable method, an adequate survey technique and SfM-MVS software allowed to obtain precise and detailed textured 3D models in automatic and easy way in all the considered case studies, despite image acquisition was done with non-professional devices such as smartphone, action camera and compact camera.

Thanks to the developed scripts, the generation of orthophotos of each façade of the considered objects and structures was quick and easy. Given the importance of a similar automatic procedure in cultural heritage documentation, such development corresponds de facto to an optimization of the overall digital documentation process in this kind of applications. Furthermore, such kind of approach eases the analysis and study of structures, objects and site of particular historical, architectural and archaeological value, by means of the easy generation of high-resolution orthophotos and 3D models. In addition, the faithful reconstruction of the objects and the determination of their exact spatial position allows further archaeological and architectural studies to be carried out on the nature of the object. For example, the three-dimensional reconstruction of a part of a column belonging to an old temple could make it possible to identify its shape and, consequently, identify the position of the piece detected with respect to the entire column. In the graphic reconstruction of architectural object and, consequently, in a two-dimensional representation, it was possible emphasize the key elements of the architecture of the surveyed structures, as shown, for example, in the Ionic capital case study.

Furthermore, this work examined the use of cameras mounted both below and above a drone: this kind of approach allowed to acquire images also in the Zenith direction for UAV photogrammetry purposes. Indeed, the developed low-cost imagery acquisition system mounted on the top of a UAV allowed acquiring visual information about the bottom part of high structures in a simple and intuitive way. The sensor chosen for such photogrammetric purpose was an action-camera, due its lightness and adequate image quality. Nevertheless, it is worth to notice that photogrammetric reconstruction to be computed with wide-angle lens cameras, such as action-cameras, required an adequate image pre-processing. Indeed, since the image formation process does not follow a central projective model, a pre-correction of the initial distortion can be applied, followed by a camera calibration procedure. In this way, it is possible to achieve, thanks to maturity, simplicity and accuracy of the software based on SfM-MVS algorithms, greater accuracy than when processing such datasets by directly applying the self-calibration method, without any prior correction of the lens distortion.

Massimiliano Pepe, <http://orcid.org/0000-0003-2508-5066>
 Domenica Costantino, <http://orcid.org/0000-0002-1909-9261>

Funding: This research was conducted with funds from the DICATEch of the Polytechnic of Bari (Italy).

Acknowledgments: We want to thank the reviewers for their careful reading of the manuscript and their constructive remarks. This research was carried out in the project: PON "Ricerca e Innovazione" 2014-2020 A. I.2 "Mobilità dei Ricercatori" D.M. n. 407-27/02/2018 AIM "Attraction and International Mobility" (AIM1895471 – Line 1)

REFERENCES

- [1] De Luca, L.: La fotomodellazione architettonica. Rilievo, modellazione, rappresentazione di edifici a partire da fotografie. Dario Flaccovio Editore, Palermo, 2011.
- [2] Murtiyoso, A.; Grussenmeyer, P.; Börlin, N.; Vandermeersch, J.; Freville, T: Open source and independent methods for bundle adjustment assessment in close-range UAV photogrammetry, *Drones*, 2(1), 2018, 3. <https://doi.org/10.3390/drones2010003>
- [3] Luhmann, T.; Robson, S.; Kyle, S.; Boehm, J.: Close-range photogrammetry and 3D imaging, Walter de Gruyter, 2007.
- [4] Smith, M. J.; Pain, C. F.: Applications of remote sensing in geomorphology, *Progress in Physical Geography*, 33(4), 2009, 568-582. <https://doi.org/10.1177/0309133309346648>
- [5] Caldera-Cordero, J. M.; Polo, M. E.: Analysis of free image-based modelling systems applied to support topographic measurements, *Survey Review*, 2018, 1-10. <https://doi.org/10.1080/00396265.2018.1451271>.
- [6] Korchenko, A. G.; Ilyash, O. S.: The generalized classification of unmanned air vehicles. In 2013 IEEE 2nd International Conference Actual Problems of Unmanned Air Vehicles Developments Proceedings (APUAVD), 2013 October, 28-34. <https://doi.org/10.1109/APUAVD.2013.6705275>
- [7] Pepe, M.; Costantino, D.; Restuccia Garofalo, A.: An Efficient Pipeline to Obtain 3D Model for HBIM and Structural Analysis Purposes from 3D Point Clouds, *Applied Sciences*, 10(4), 2020, 1235. <https://doi.org/10.3390/app10041235>
- [8] Apollonio, F. I.; Ballabeni, M.; Gaiani, M.: Color enhanced pipelines for reality-based 3D modeling of on-site medium sized archeological artifacts, *Virtual Archaeology Review*, 5(10), 2014, 59-76. <https://doi.org/10.4995/var.2014.4218>
- [9] Ullman, S.: The interpretation of structure from motion, *Proceedings of the Royal Society of London, Series B. Biological Sciences*, 203(1153), 1979, 405-426. <https://doi.org/10.1098/rspb.1979.0006>
- [10] Snavely, N.; Seitz, S. M.; Szeliski, R.: Photo tourism: exploring photo collections in 3D, *ACM Transactions on Graphics*, 25(3), 2006, 835-846. <https://doi.org/10.1145/1141911.1141964>
- [11] Jaud, M.; Passot, S.; Allemand, P.; Le Dantec, N.; Grandjean, P.; Delacourt, C.: Suggestions to Limit Geometric Distortions in the Reconstruction of Linear Coastal Landforms by SfM Photogrammetry with PhotoScan® and MicMac® for UAV Surveys with Restricted GCPs Pattern, *Drones*, 3(1), 2019, 2. <https://doi.org/10.3390/drones3010002>
- [12] Alt, N.; Rives, P.; Steinbach, E.: Reconstruction of transparent objects in unstructured scenes with a depth camera, In 2013 IEEE International Conference on Image Processing, 2013, 4131-4135. <https://doi.org/10.1109/ICIP.2013.6738851>
- [13] Ihrke, I.; Kutulakos, K. N.; Lensch, H. P.; Magnor, M.; Heidrich, W.: Transparent and specular object reconstruction, In *Computer Graphics Forum*, 29(8), 2010, 2400-2426. <https://doi.org/10.1111/j.1467-8659.2010.01753.x>

- [14] Peña-Villasenín, S.; Gil-Docampo, M.; Ortiz-Sanz, J.: 3-D Modeling of Historic Façades Using SFM Photogrammetry Metric Documentation of Different Building Types of a Historic Center, *International Journal of Architectural Heritage*, 11(6), 2017, 871-890. <https://doi.org/10.1080/15583058.2017.1317884>
- [15] Peña-Villasenín, S.; Gil-Docampo, M.; Ortiz-Sanz, J.: Desktop vs cloud computing software for 3D measurement of building façades: The monastery of San Martín Pinario, *Measurement*, 2020, 149, 106984. <https://doi.org/10.1016/j.measurement.2019.106984>
- [16] Snavely N.: Scene reconstruction and visualization from internet photo collections, PhD thesis, 2008.
- [17] Bianco, S.; Ciocca, G.; Marelli, D.: Evaluating the performance of structure from motion pipelines. *Journal of Imaging*, 4(8), 2018, 98. <https://doi.org/10.3390/jimaging4080098>
- [18] Lowe D. G.: Distinctive image features from scale-invariant keypoints. *IJCV*, 2004. <https://doi.org/10.1023/B:VISI.0000029664.99615.94>
- [19] Masiero, A.; Vettore, A.: Improved feature matching for mobile devices with IMU, *Sensors*, 16(8), 2016, 1243. <https://doi.org/10.3390/s16081243>
- [20] Fischler, M.; Bolles, R.: Random sample consensus: A paradigm for model fitting with applications to image analysis and automated cartography, *Readings in Computer Vision: Issues, Problems, Principles, and Paradigms*, 1987, 726–740. <https://doi.org/10.1016/B978-0-08-051581-6.50070-2>
- [21] Pepe, M.; Fregonese, L.; Crocetto, N.: Use of SfM-MVS approach to nadir and oblique images generated through aerial cameras to build 2.5D map and 3D models in urban areas, *Geocarto International*, 2019. <https://doi.org/10.1080/10106049.2019.1700558>
- [22] Fraser, C. S.: Digital camera self-calibration, *ISPRS Journal of Photogrammetry and Remote sensing* 52(4), 1997, 149-159. [https://doi.org/10.1016/S0924-2716\(97\)00005-1](https://doi.org/10.1016/S0924-2716(97)00005-1)
- [23] Triggs, B.; McLauchlan, P. F.; Hartley, R. I.; Fitzgibbon, A. W.: Bundle adjustment—a modern synthesis. In *Vision algorithms: theory and practice*, Springer Berlin Heidelberg, 2000, 298-372. https://doi.org/10.1007/3-540-44480-7_21
- [24] Indelman, V.; Roberts, R.; Beall, C.; Dellaert, F.: Incremental light bundle adjustment. *Proceedings of the British Machine Vision Conference (BMVC 2012)*, 2012, 3-7. <https://doi.org/10.5244/C.26.134>
- [25] Gerke, M.; Przybilla, H. J.: Accuracy analysis of photogrammetric UAV image blocks: Influence of onboard RTK-GNSS and cross flight patterns, *Photogrammetrie-Fernerkundung-Geoinformation*, 1, 2016, 17-30. <https://doi.org/10.1127/pfg/2016/0284>
- [26] Fraser, C. S.: Automatic camera calibration in close range photogrammetry, *Photogrammetric Engineering & Remote Sensing*, 79(4), 2013, 381-388. <https://doi.org/10.14358/PERS.79.4.381>
- [27] Brown, D.C.: Close-Range Camera Calibration, *Photogrammetric Engineering*, 37(8), 1971, 855–866.
- [28] Furukawa, Y.; Ponce, J.: Accurate, dense, and robust multi-view stereopsis, *Trans. Pattern Anal. Mach. Intell.*, 32, 2010, 1362–1376. <https://doi.org/10.1109/TPAMI.2009.161>
- [29] Kolev K.; Brox T.; Cremers D.: Fast Joint Estimation of Silhouettes and Dense 3D Geometry from Multiple Images, *Transactions on Pattern Analysis and Machine Intelligence*, 2012, 34(3), 2012, 493–505. <https://doi.org/10.1109/TPAMI.2011.150>
- [30] Goesele M.; Snavely N.; Curless B.; Hoppe H.; Seitz S.: Multi-View Stereo for Community Photo Collections, In *International Conference on Computer Vision*, 3(6), 2007, 1–8. <https://doi.org/10.1109/ICCV.2007.4408933>
- [31] Tsai, V. J.: Delaunay triangulations in TIN creation: an overview and a linear-time algorithm, *International Journal of Geographical Information Science*, 7(6), 1993, 501-524. <https://doi.org/10.1080/02693799308901979>
- [32] Si, H.: TetGen, a Delaunay-based quality tetrahedral mesh generator, *ACM Transactions on Mathematical Software*, 41(2), 2015, 11. <https://doi.org/10.1145/2629697>
- [33] Remondino, F.: Worth a thousand words – photogrammetry for archaeological 3D surveying, in: *Opitz, R.S.* 2006.

- [34] McCarthy, J.: Recursive functions of symbolic expressions and their computation by machine, 1959.
- [35] Holtz, N. M.; Rasdorf, W. J.: LISP-A CAD system programming language, *Journal of Technical Topics in Civil Engineering*, 109(1), 1983, 58-72.
- [36] Kraus, K.: *Photogrammetry: geometry from images and laser scans*, Walter de Gruyter, 2011.
- [37] Sassu, R.: *Culti primari e secondari nel santuario urbano di Metaponto, Thiasos*, 2, 2013, 3-18.
- [38] Parker, J. R.: *Algorithms for image processing and computer vision*, John Wiley & Sons, 2010.
- [39] Adami, A.; Fregonese, L.; Gallo, M.; Helder, J.; Pepe, M.; Treccani, D.: Ultra-light UAV systems for the metrical documentation of cultural heritage: applications for architecture and archaeology, *Int. Arch. Photogramm. Remote Sens. Spatial Inf. Sci.*, 2019, XLII-2/W17, 15-21. <https://doi.org/10.5194/isprs-archives-XLII-2-W17-15-2019>
- [40] Fusiello, A.: Uncalibrated Euclidean reconstruction: a review, *Image and Vision Computing*, 18(6-7), 2000, 555-563. [https://doi.org/10.1016/S0262-8856\(99\)00065-7](https://doi.org/10.1016/S0262-8856(99)00065-7)
- [41] CloudCompare Available online: <http://www.cloudcompare.org/>, Version 2.6.2, [GPL software], 2016.
- [42] Pepe, M.; Fregonese, L.; Scaioni, M.: Planning airborne photogrammetry and remote sensing missions with modern platforms and sensors, *European Journal of Remote Sensing*, 51(1), 2018, 412-436. <https://doi.org/10.1080/22797254.2018.1444945>